Available online at http://scik.org
Commun. Math. Biol. Neurosci. 2023, 2023:75
https://doi.org/10.28919/cmbn/8031
ISSN: 2052-2541

A COMPREHENSIVE STUDY OF OPTIMAL CONTROL MODEL SIMULATION FOR COVID-19 INFECTION WITH RESPECT TO MULTIPLE VARIANTS

A. VENKATESH[1,*], M. ANKAMMA RAO[1], D. K. K. VAMSI[2]

[1]Department of Mathematics, AVVM Sri Pushpam College (Affiliated to Bharathidasan University), Poondi, Thanjavur (Dt), Tamilnadu-613 503, India

[2]Department of Mathematics and Computer Science, Sri Sathya Sai Institute of Higher Learning-SSSIHL, Puttaparthi (Dt), Andhra Pradesh-515134, India

Abstract. The COVID-19 virus is still spreading around the world. Several SARS-CoV-2 variants have been identified during this COVID-19 pandemic. In this study, we present a compartmental mathematical model using ordinary differential equations to investigate the impact of four different SARS-CoV-2 variants on the transmission of SARS-CoV-2 across India. The proposed mathematical model incorporates the alpha variant, beta variant, gamma variant, and delta variant subpopulations apart from the typical susceptible, exposed, recovered, and dead subpopulations. As part of the India pandemic, we used the model to determine the basic reproduction number (R_0) and the daily rates of infection, death, and recovery for each strain. Sensitivity analysis is employed to comprehend the influence of estimated parameter values on the number of infections that result in four variants. Then, using vaccine and therapy as the control variables, we define and analyse an optimum control problem. These optimal controls are described by the Pontryagin's Minimal Principle. Results showed that the combination of vaccination and treatment strategies was most efficient in minimizing infection and enhancing recovery. The cost-effectiveness analysis is used to determine the best control strategy to minimize infected individuals.

Keywords: four-strain COVID-19 model; sensitive analysis; optimal control problem; cost effectiveness analysis.
2020 AMS Subject Classification: 37N25, 35F21.

*Corresponding author
E-mail address: avenkateshmaths@gmail.com
Received May 26, 2023

1. INTRODUCTION

One of the deadliest and most severe pandemics in recent history is the SARS-CoV-2 pandemic, which was driven by the SARS-CoV-2 infection. Around 6.28 million COVID-19 deaths and over half a billion confirmed SARS-CoV-2 cases were reported by the WHO [1] by May 2022, more than two years after the virus's first documented pandemic in December 2019. There have been multiple waves of the SARS-CoV-2 pandemic. These waves are mostly carried by the reduction of non-pharmaceutical therapies and the development of novel variants of concern (VOCs). Some SARS-CoV-2 variants are more contagious and severe in populations than others variants. The World Health Organization (WHO) and the Centers for Disease Control and Prevention (CDC) [2] have classified the SARS-CoV-2 variants into three categories [3] 1) a variant of concern 2) a variant of interest and 3) a variant of high consequence variant of concern: The SARS-CoV-2 alpha, beta, gamma, delta, and omicron variants are categorized as a variant of concern (VOCs.). These variations have a higher propensity to lead to severe illness, avoid detection by tests, or resist antiviral therapy. In those who have had vaccinations or have already contracted an infection, VOC is more contagious and more likely to result in reinfections or emerging infections.

According to the World Health Organization, the alpha variant [4], formerly known as B.1.1.7, was first discovered in the UK in September 2020, and by December 2020, it had arrived in the US. The World Virus Network claims that at least 114 nations have been affected by its proliferation. Around 60% of all SARS-COV-2 cases were caused by alpha. The beta variant[5], formerly known as B.1.351, was initially identified as a variety of concerns in December 2020 after being found in South Africa in May 2020. Eight different mutations exist in it, and these can alter how the virus infects human cells. According to Global Virus Network, it has propagated to at least 48 nations and 23 US states. The gamma variation[6], commonly known as P.1, first emerged in Brazil in November 2020. At the beginning of January 2021, four passengers who had visited Brazil tested positive for the gamma variant in Japan. This variant has been spotted in 74 different countries, according to the United Nations website. The delta variant [7], formerly known as B.1.617.2, initially emerged in India in October 2020 and was categorized as a variant of concern in May 2021. Over a short period, the Delta variant

had reached more than 100 nations and had taken over as the worldwide standard. omicron variant [8], also known as B.1.1.529, is a brand-new, severely mutated SARS-CoV-2 variant that the World Health Organization has now classified as a VOC as of November 26, 2021. The omicron variety was the first to be discovered in South Africa. Now it has been discovered in at least 24 countries. A variant of Interest (VOIs) : The Epsilon (American), Zeta (Brazilian), Eta (many countries), Theta (Philippines), Lota (American), Kappa (Indian), and Lambda (Peruvian) variants of the SARS-CoV-2 coronavirus are recognized as variations of interests. These variants have genetic traits that, in contrast to earlier forms of the virus, indicate higher transmissibility, resistance to treatment or diagnostics, or more severe illness. A variant of high consequence: Current vaccines do not protect the variation known as VOI. There are currently no highly significant SARS-CoV-2 mutations. To analyze and comprehend the dynamics of various outbreaks in different regions of the world, mathematical models are helpful and have been utilized extensively[9, 10, 11]. Researchers have concentrated their attention on several mathematical compartmental models, whether stochastic[12, 13] or deterministic in order to explore the spread of SARS-COV-2, including the influence of the numerous SARS-CoV-2 variants on this spread, and to propose strategies to slow this spread. Most mathematical models study one single variant and examine the effects of vaccination [14, 15], hospitalization, and quarantine [16, 17], as well as the effects on various age groups [18, 19]. Many mathematical models have been developed in recent months to examine the impact of several variants on the spread of SARSCoV-2 when it became apparent how important distinct VOCs were in the rapid rise in the number of SARS-CoV-2 cases in various regions. Yagan et al. [20] investigated the efficiency of mask use in preventing the spread of COVID-19 in the context of viral mutations using network models. Arrude et al [21] developed an SEIR model with multiple viral strains and reinfection because of waning immunity. They compared the cost of infection control (lockdown) to the cost of increased infection levels in the healthcare system over two years as they evaluated time-varying control tactics in the context of lockdown measures. Using symptomatic and asymptomatic individuals, Mathilde Massard et al [22] constructed a multi-strain epidemic model SARS-CoV-2 by using French data. To further understand the SARS-CoV-2 transmission in Columbia, Gonzal et al.[23] expanded a two-strain SEIR model

to include asymptomatic, hospitalized, and deceased people. The research analyzes the global stability of a two-strain SEIR model with two general incidence rates, as well as a multi-strain SEIR model with saturated incidence and treatment controls as in [24], which also addresses an optimal control problem. In order to determine the best optimal strategies for reducing the number of people infected with the various SARS-COV-2 variants, I Abdel Hak essounaini et al [25] built a multi-strain model that included four SARS-COV-2 variants. Using the combination of vaccination and treatment controls, Ririt Andria Sari et al developed an SVEIR model with a single variant [26] and Bouchaib Khajji et al. [27] constructed a two-strain model to determine the best control approach. The most efficient way to stop any infectious disease is by immunization. It is predicted that the vaccine programme [28] will avert about 2-3 million fatalities annually. The effectiveness of SARS-CoV-2 vaccines is up to 95% in reducing symptomatic SARS-CoV-2 diseases. The Oxford-AstraZeneca (Covishield)and Covaxin vaccines were first approved in India. The Covaxin, manufactured by Bharat Biotech in partnership with the Indian Council of Medical Research, has a 78% effectiveness rate [29] and The vaccination Covishield, a version of OxfordAstraZeneca's (ChAdOx1 nCoV-19), achieved a 67% effectiveness rate [30]. Influenced by the importance of multistrain SARS-CoV-2 models and their scarcity, we developed a novel multistrain model (S$E_1E_2E_3E_4I_1I_2I_3I_4$HRD model) by incorporating SARS-COV-2 alpha, beta, gamma, and delta variants. One of the main concerns of policymakers, health authorities, and the government is the best use of control measures like vaccinations or medicines. In order to minimize the infected population we present an optimal control strategy associated with two kinds of controls. The first control signifies the vaccination control on the susceptible population and the second control characterizes the treatment control on the symptomatic infected population.

The article is structured as follows: We present an original mathematical model in Section 2 that depicts the dynamics of the population and the spread of the SARS-COV-2 variants. We calculated the fundamental reproduction number and performed stability of the disease-free equilibrium in Section 3. Using daily cumulative confirmed cases, we calibrated our mathematical model in in section 4 and sensitive analysis was also performed for model parameters of each strain in section 5. we investigate the optimal control technique for the recommended model.

Pontryagin's maximum principle is employed to identify these optimal controls in section. The behavior of the system in the presence of four variants, both with and without mitigation is displayed in section 6. Finally, section 7 brings the article to a conclusion.

2. Mathematical Model With Four SARS-CoV-2 Variants

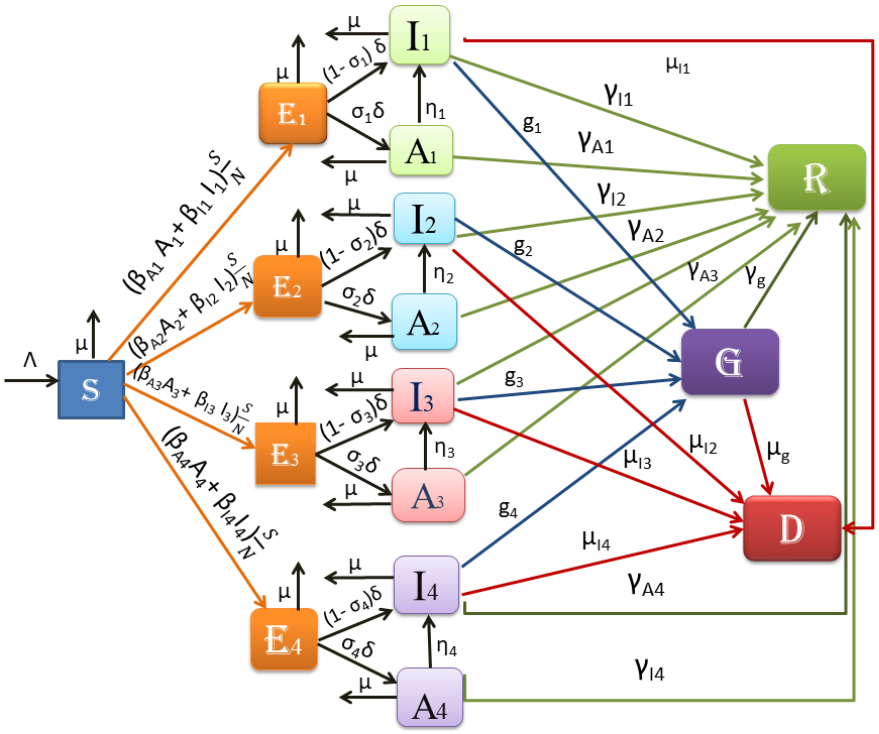

FIGURE 1. Schematic diagram of the sixteen compartments in the model

In this section, we propose a compartmental mathematical model to study the spread of four SARS-COV-2 variants in India. This mathematical model has 16 compartments: the number of individuals susceptible to the infection at time t S(t); the number of individuals exposed to alpha, beta, gamma, and delta variants at time t, $E_1(t)$, $E_2(t)$, $E_3(t)$ and $E_4(t)$; the number of asymptomatic individuals with alpha, beta, gamma and delta variants at time t, $I_1(t)$, $I_2(t)$, $I_3(t)$ and $I_4(t)$; the number of symptomatic individuals with alpha, beta, gamma and delta variants at time t, $I_1(t)$, $I_2(t)$, $I_3(t)$ and $I_4(t)$; the number of individuals hospitalized due to severe illness at time t, H(t); the number of individuals recovered against infection at time t, R(t), and number of individuals deceased with infection at time t, D(t).

Compartment S defines the population of susceptible people who are not infected but can become ill. The recruitment rate denoted as Λ increases this compartment whereas the natural death rate μ decreases it. As a result of its effective contact with those asymptomatic infected and smptomatic infected individuals with the SARS-COV-2 i^{th} variant at a rates of β_{A_i} and β_{I_i}, it is diminished by the rates β_{A_i} and β_{I_i}. Therefore

$\frac{dS}{dt} = \Lambda - \sum_{i=1}^{4}(\beta_{A_i}A_i + \beta_{I_i}I_i)\frac{S}{N} - \mu S$

Compartment $\mathbf{E_i}$ consists of those who have been exposed to the virus and are symptomless carriers of the virus, with the potential to transmit the disease and become symptomatic infection. It is increases by susceptible S(t) individuals who are exposed at the rates β_{A_i} and β_{I_i} and also decreases by natural rate μ. A portion σ_i of exposed individuals becomes asymptomatic infected SARS-CoV-2 variant and remaining portion $(1-\sigma_i)$ becomes symptomtic infected with SARS-CoV-2 variant at a rate δ. It is also reduced by natural death rate μ. So that

$\frac{dE_i}{dt} = (\beta_{A_i}A_i + \beta_{I_i}I_i)\frac{S}{N} - (\mu+\delta)E_i$

Compartment $\mathbf{A_i}$ depicts individuals who are infected with SARS-CoV-2 variant but does not shows any symptoms. It increases in size as the proportion σ_i of exposed individuals becomes asymptomatic infected with SARS-CoV-2 variant at a rate δ. It diminishes by the rate η_i as the number of asymptomatic infected individuals becomes symptomatic at the rate η_i and also declines as some of them recover at a rate of γ_{A_i}. Furthermore, this class experiences a reduction by the natural mortality rate μ. Therefore

$\frac{dA_i}{dt} = \sigma_i\delta E_i - (\gamma_{A_i} + \eta_i + \mu)A_i$

Compartment $\mathbf{I_i}$ involves the individuals who are infected with SARS-CoV-2 variant and have symptoms. This population increases at the rate δ as the remaining $(1-\sigma_i)$ portion of exposed individuals becomes symptomatic infected with SARS-CoV-2 variant at the rate δ and also increases by the rate η_i at which the asymptomatic individuals becomes symptomatic infected. It diminishes by g_i as the number of infected individuals admitted to hospitals at a rate of g_i due to serious illnesses and also declines as some of them recover at a rate of γ_{I_i}. Furthermore, this class diminished by the both natural mortality rate μ and the infectious mortality rate μ_i caused by the SARS-CoV-2 variant. Hence

$\frac{dI_i}{dt} = (1-\sigma_i)\delta E_i + \eta_i A_i - (g_i + \gamma_{I_i} + \mu_i + \mu)I_i$

Compartment G represents individuals who are in hospitals because of a severe infection. It increases by the rate g_i as symptomatic infected individuals with SARS-CoV-2 variant joins hospital at a rate of g_i. It declines by both the natural mortality rate μ and the symptomatic infected with SARS-CoV-2 variant death rate μ_g As a result,

$\frac{dG}{dt} = \sum_{i=1}^{4} g_i I_i - (\gamma_g + \mu_g + \mu)G$

Compartment R includes of those who have recovered from the SARS-CoV-2 variant. It becomes larger at the rates γ_{A_i} and γ_{I_i} as the infected individuals with SARS-CoV-2 variant recovered by the rates γ_{A_i} and γ_{I_i} and also increases by the rate γ_h at which the hospitalised individuals are recovered. Furthermore it reduces by natural death rate μ. Therefore

$\frac{dR}{dt} = \sum_{i=1}^{4}(\gamma_{A_i} A_i + \gamma_{I_i} I_i) + \gamma_g G - \mu R$

Compartment D contains individuals who passed away as a result of severe infection or treatment that was ineffective. It increases by a mortality rate μ_i of symptomatic infected individuals with SARS-CoV-2 variant and also rises by mortality rate μ_g of hospitalization individuals. So that $\frac{dD}{dt} = \sum_{i=1}^{4} \mu_i I_i + +\mu_g G$

The Schematic diagram in Figure.1 depicts the proposed model. Using our assumptions and Schematic diagram, the system of nonlinear differential equations for the model of SARS-CoV-2 variants can be obtained as follows:

$$
\begin{aligned}
\frac{dS}{dt} &= \Lambda - \sum_{i=1}^{4}(\beta_{A_i} A_i + \beta_{I_i} I_i)\frac{S}{N} - \mu S \\
\frac{dE_i}{dt} &= (\beta_{A_i} A_i + \beta_{I_i} I_i)\frac{S}{N} - (\mu + \delta)E_i \\
\frac{dA_i}{dt} &= \sigma_i \delta E_i - (\gamma_{A_i} + \eta_i + \mu)A_i \\
\frac{dI_i}{dt} &= (1-\sigma_i)\delta E_i + \eta_i A_i - (g_i + \gamma_{I_i} + \mu_i + \mu)I_i \\
\frac{dG}{dt} &= \sum_{i=1}^{4} g_i I_i - (\gamma_g + \mu_g + \mu)G \\
\frac{dR}{dt} &= \sum_{i=1}^{4}(\gamma_{A_i} A_i + \gamma_{I_i} I_i) + \gamma_g G - \mu R \\
\frac{dD}{dt} &= \sum_{i=1}^{4} \mu_i I_i + +\mu_g G
\end{aligned}
\tag{1}
$$

with the initial conditions

$$S(0) \geq 0, E_i(0) \geq 0, A_i(0) \geq 0, I_i(0) \geq 0, G(0) \geq 0, R(0) \geq 0 \& D(0) \geq 0 \tag{2}$$

The total human population N(t) at time t is specified by

$N(t) = S(t) + E_1(t) + E_2(t) + E_3(t) + E_4(t) + A_1(t) + A_2(t) + A_3(t) + A_4(t) + I_1(t) + I_2(t) +$
$I_3(t) + I_4(t) + G(t) + R(t) + D(t)$.

3. Model Analysis

3.1 Positivity on the solutions

Theorem 1.

$\Omega = \{(S(t), E_1(t), A_1(t), I_1(t), E_2(t), A_2(t), I_2(t), E_3(t), A_3(t), I_3(t), E_4(t), A_4(t), I_4(t), G(t), R(t),$
$D(t)) \in \mathbb{R}^{16}_+ : 0 \leq (S, E_1, A_1, I_1, E_2, A_2, I_2, E_3, A_3, I_3, E_4, A_4, I_4, G, R, D) \leq \frac{\Lambda}{\mu}\}$

is positive invariant and an attracting set for system (1) if the initial conditions (2) holds.

proof. From the system (1), we have

$\frac{ds}{dt} = \Lambda - (\sum_{i=1}^{4}(\beta_{A_i} A_i + \beta_{I_i} I_i)\frac{1}{N} + \mu)S$

Let ψ(t)=$(\sum_{i=1}^{4}(\beta_{A_i} A_i + \beta_{I_i} I_i)\frac{1}{N} + \mu)$

Then $\frac{ds}{dt} + \psi S \geq 0$

Multiplying above equation with $\exp(\int_0^t \psi(s)\,ds)$,we get

$\frac{ds}{dt}\exp(\int_0^t \psi(s)\,ds) + \psi(t)S(t)\exp(\int_0^t \psi(s)\,ds) \geq 0$

$\Rightarrow \frac{d}{dt}[S(t)\exp(\int_0^t \psi(s)\,ds)] \geq 0$

Integrating on both sides, we get

$S(t) \geq S(0)exp(-\int_0^t \psi(s)\,ds) \geq 0$

Therefore $S(t) \geq 0$ for all $t > 0$

From the system (1) we have

$\frac{dE_i}{dt} = (\beta_i I_i)\frac{S}{N} + (\mu + \delta_i)E_i$ for i=1,2,3,4

Let $\Phi(t) = (\mu + \delta_i)$

Then $\frac{dE_i}{dt} + \Phi E_i(t) \geq 0$

Multiplying above equation with $\exp(\int_0^t \Phi(s)\,ds)$,we get

$\frac{dE_i}{dt}\exp(\int_0^t \Phi(s)\,ds) + \Phi(t)E_i(t)\exp(\int_0^t \Phi(s)\,ds) \geq 0$

$\Rightarrow \frac{d}{dt}[E_i(t)\exp(\int_0^t \Phi(s)\,ds)] \geq 0$

Integrating on both sides, we get

$E_i(t) \geq E_i(0)exp(-\int_0^t \phi(s)\,ds) \geq 0$

Therefore $E_i(t) \geq 0$ for all $t > 0$ and for i=1,2,3,4

Consequently, from the system (1), we have

$\frac{dA_i}{dt} = \sigma_i \delta E_i - (\gamma_{A_i} + \eta_i + \mu)A_i$

Let $\chi(t) = \gamma_{A_i} + \eta_i + \mu$. Then

$\frac{dA_i}{dt} + \chi A_i = 0$ for i =1,2,3,4.

Multiplying above equation with $\exp(\int_0^t \chi(s)\,ds)$,we get

$\frac{dA_i}{dt}\exp(\int_0^t \chi(s)\,ds) + \chi(t)A_i(t)\exp(\int_0^t \chi(s)\,ds) \geq 0$

$\Rightarrow \frac{d}{dt}[A_i(t)\exp(\int_0^t \chi(s)\,ds)] \geq 0$

Hence $A_i(t) \geq 0$ for all $t > 0$ for i=1,2,3,4

Similarly the following inequalities can be easily obtained from the other equations of the system (1)

$I_i(t) \geq I_i(0)exp(-\int_0^t (g_i + \gamma_{I_i} + \mu_i + \mu)(s)\,ds) \geq 0$ for i=1,2,3,4

$G(t) \geq G(0)exp(-\int_0^t (\gamma_g + \mu_g + \mu)(s)\,ds) \geq 0$ and

$R(t) \geq R(0)exp(-\int_0^t \mu(s)\,ds) \geq 0.$

Since each $I_i(t) \geq 0$ and $G(t) \geq 0$, we have $D(t) \geq 0$

we have $N(t) = S(t) + E_1(t) + E_2(t) + E_3(t) + E_4(t) + A_1(t) + A_2(t) + A_3(t) + A_4(t) + I_1(t) +$

$I_2(t) + I_3(t) + I_4(t) + G(t) + R(t) + D(t)$

differentiating N(t) with respect to t, and adding all equations in system(1)we get

$\frac{dN}{dt} = \Lambda - \mu N$

$\Rightarrow \frac{dN}{dt} + \mu N = \Lambda$

After solving we get

$N(t) = \frac{\Lambda}{\mu} + (N(0) - \frac{\Lambda}{\mu})e^{-\mu t}$ for $t \geq 0$

If $N(0) = \frac{\Lambda}{\mu}$ then $N(t) = \frac{\Lambda}{\mu}$

if $N(0) > \frac{\Lambda}{\mu}$, then N(t) asymptotically approaches $\frac{\Lambda}{\mu}$ as $t \to \infty$.

Hence the solution set Ω of model (1) is positively invariant and constrained.

3.2 Basic reproduction number ($\mathbf{R_0}$)

The average number of secondary infections produced by single primary infection throughout

the course of the infectious period in a totally susceptible population is known as the basic reproduction number (R_0). The next-generation matrix approach [31, 32] is used to describe the algebraic expression of R_0 for system (2). Let $\mathscr{F}$ represent the derivatives of new infections and let $\mathscr{V}$ represent the individual transfers to compartments.

Then

$$\mathscr{F} = \begin{pmatrix} (\beta_{A_1}A_1+\beta_{I_1}I_1)\frac{S}{N} \\ 0 \\ 0 \\ (\beta_{A_2}A_2+\beta_{I_{12}}I_2)\frac{S}{N} \\ 0 \\ 0 \\ (\beta_{A_3}A_3+\beta_{I_3}I_3)\frac{S}{N} \\ 0 \\ 0 \\ (\beta_{A_4}A_4+\beta_{I_4}I_4)\frac{S}{N} \\ 0 \\ 0 \end{pmatrix} \quad \& \quad \mathscr{V} = \begin{pmatrix} (\mu+\delta)E_1 \\ -\sigma_1\delta E_1+(\gamma_{A_1}+\eta_1+\mu)A_1 \\ -(1-\sigma_1)\delta E_1-\eta_1A_1+(g_1+\gamma_{I_1}+\mu_1+\mu)I_1 \\ (\mu+\delta)E_2 \\ -\sigma_3\delta E_3+(\gamma_{A_3}+\eta_3+\mu)A_3 \\ -(1-\sigma_3)\delta E_3-\eta_3A_3+(g_3+\gamma_{I_3}+\mu_3+\mu)I_3 \\ (\mu+\delta)E_3 \\ -\sigma_3\delta E_3+(\gamma_{A_3}+\eta_3+\mu)A_3 \\ -(1-\sigma_3)\delta E_3-\eta_3A_3+(g_3+\gamma_{I_3}+\mu_3+\mu)I_3 \\ (\mu+\delta)E_4 \\ -\sigma_4\delta E_4+(\gamma_{A_4}+\eta_4+\mu)A_4 \\ -(1-\sigma_4)\delta E_4-\eta_4A_4+(g_4+\gamma_{I_4}+\mu_4+\mu)I_4 \end{pmatrix}.$$

Now the Jacobian matrices of $\mathscr{F}$ and $\mathscr{V}$ can be written as

$$F = \begin{pmatrix} 0 & \frac{\beta_{A_1}\Lambda}{\mu} & \frac{\beta_{I_1}\Lambda}{\mu} & 0 & 0 & 0 & 0 & 0 & 0 & 0 & 0 & 0 \\ 0 & 0 & 0 & 0 & 0 & 0 & 0 & 0 & 0 & 0 & 0 & 0 \\ 0 & 0 & 0 & 0 & 0 & 0 & 0 & 0 & 0 & 0 & 0 & 0 \\ 0 & 0 & 0 & 0 & \frac{\beta_{A_2}\Lambda}{\mu} & \frac{\beta_{I_2}\Lambda}{\mu} & 0 & 0 & 0 & 0 & 0 & 0 \\ 0 & 0 & 0 & 0 & 0 & 0 & 0 & 0 & 0 & 0 & 0 & 0 \\ 0 & 0 & 0 & 0 & 0 & 0 & 0 & 0 & 0 & 0 & 0 & 0 \\ 0 & 0 & 0 & 0 & 0 & 0 & 0 & \frac{\beta_{A_3}\Lambda}{\mu} & \frac{\beta_{I_3}\Lambda}{\mu} & 0 & 0 & 0 \\ 0 & 0 & 0 & 0 & 0 & 0 & 0 & 0 & 0 & 0 & 0 & 0 \\ 0 & 0 & 0 & 0 & 0 & 0 & 0 & 0 & 0 & 0 & 0 & 0 \\ 0 & 0 & 0 & 0 & 0 & 0 & 0 & 0 & 0 & 0 & \frac{\beta_{A_4}\Lambda}{\mu} & \frac{\beta_{I_4}\Lambda}{\mu} \\ 0 & 0 & 0 & 0 & 0 & 0 & 0 & 0 & 0 & 0 & 0 & 0 \\ 0 & 0 & 0 & 0 & 0 & 0 & 0 & 0 & 0 & 0 & 0 & 0 \end{pmatrix}$$

$$V = \begin{pmatrix} -(\mu+\delta) & 0 & 0 & 0 & 0 & 0 & 0 & 0 & 0 & 0 & 0 & 0 \\ \sigma_1\delta & -X_1 & 0 & 0 & 0 & 0 & 0 & 0 & 0 & 0 & 0 & 0 \\ (1-\sigma_1)\delta & \eta_1 & -Y_1 & 0 & 0 & 0 & 0 & 0 & 0 & 0 & 0 & 0 \\ 0 & 0 & 0 & -(\mu+\delta) & 0 & 0 & 0 & 0 & 0 & 0 & 0 & 0 \\ 0 & 0 & 0 & \sigma_2\delta & -X_2 & 0 & 0 & 0 & 0 & 0 & 0 & 0 \\ 0 & 0 & 0 & (1-\sigma_2)\delta & \eta_2 & -Y_2 & 0 & 0 & 0 & 0 & 0 & 0 \\ 0 & 0 & 0 & 0 & 0 & 0 & -(\mu+\delta) & 0 & 0 & 0 & 0 & 0 \\ 0 & 0 & 0 & 0 & 0 & 0 & \sigma_3\delta & -X_3 & 0 & 0 & 0 & 0 \\ 0 & 0 & 0 & 0 & 0 & 0 & (1-\sigma_3)\delta & \eta_3 & -Y_3 & 0 & 0 & 0 \\ 0 & 0 & 0 & 0 & 0 & 0 & 0 & 0 & 0 & -(\mu+\delta) & 0 & 0 \\ 0 & 0 & 0 & 0 & 0 & 0 & 0 & 0 & 0 & \sigma_4\delta & -X_4 & 0 \\ 0 & 0 & 0 & 0 & 0 & 0 & 0 & 0 & 0 & (1-\sigma_4)\delta & \eta_4 & -Y_4 \end{pmatrix}.$$

Where $X_i = (\gamma_{A_i} + \eta_i + \mu)$ $Y_i = (g_i + \gamma_{I_i} + \mu_i + \mu)$ for i = 1,2,3,4.

$$FV^{-1} = \begin{pmatrix} R_{01} & \frac{\beta_{A_1}\Lambda}{X_1\mu} & \frac{\beta_{I_1}\Lambda}{Y_1\mu} & 0 & 0 & 0 & 0 & 0 & 0 & 0 & 0 & 0 \\ 0 & 0 & 0 & 0 & 0 & 0 & 0 & 0 & 0 & 0 & 0 & 0 \\ 0 & 0 & 0 & 0 & 0 & 0 & 0 & 0 & 0 & 0 & 0 & 0 \\ 0 & 0 & 0 & R_{02} & \frac{\beta_{A_2}\Lambda}{X_2\mu} & \frac{\beta_{I_2}\Lambda}{Y_2\mu} & 0 & 0 & 0 & 0 & 0 & 0 \\ 0 & 0 & 0 & 0 & 0 & 0 & 0 & 0 & 0 & 0 & 0 & 0 \\ 0 & 0 & 0 & 0 & 0 & 0 & 0 & 0 & 0 & 0 & 0 & 0 \\ 0 & 0 & 0 & 0 & 0 & 0 & R_{03} & \frac{\beta_{A_3}\Lambda}{X_3\mu} & \frac{\beta_{I_3}\Lambda}{Y_3\mu} & 0 & 0 & 0 \\ 0 & 0 & 0 & 0 & 0 & 0 & 0 & 0 & 0 & 0 & 0 & 0 \\ 0 & 0 & 0 & 0 & 0 & 0 & 0 & 0 & 0 & 0 & 0 & 0 \\ 0 & 0 & 0 & 0 & 0 & 0 & 0 & 0 & 0 & R_{04} & \frac{\beta_{A_4}\Lambda}{X_4\mu} & \frac{\beta_{I_4}\Lambda}{Y_4\mu} \\ 0 & 0 & 0 & 0 & 0 & 0 & 0 & 0 & 0 & 0 & 0 & 0 \\ 0 & 0 & 0 & 0 & 0 & 0 & 0 & 0 & 0 & 0 & 0 & 0 \end{pmatrix}$$

where

$$R_{01} = \frac{\sigma_1\delta\beta_{A_1}\Lambda}{\mu(\mu+\delta)(\gamma_{A_1}+\eta_1+\mu)} + \frac{\beta_{I_1}\Lambda(\sigma_1\delta\eta_1-(1-\sigma_1)\delta(\gamma_{A_1}+\eta_1+\mu))}{\mu(\mu+\delta)(\gamma_{A_1}+\eta_1+\mu)(g_1+\gamma_{I_1}+\mu_1+\mu)}$$

$$R_{02} = \frac{\sigma_2\delta\beta_{A_2}\Lambda}{\mu(\mu+\delta)(\gamma_{A_2}+\eta_2+\mu)} + \frac{\beta_{I_2}\Lambda(\sigma_2\delta\eta_2-(1-\sigma_2)\delta(\gamma_{A_2}+\eta_2+\mu))}{\mu(\mu+\delta)(\gamma_{A_2}+\eta_2+\mu)(g_2+\gamma_{I_2}+\mu_2+\mu)}$$

$$R_{03} = \frac{\sigma_3\delta\beta_{A_3}\Lambda}{\mu(\mu+\delta)(\gamma_{A_3}+\eta_3+\mu)} + \frac{\beta_{I_3}\Lambda(\sigma_3\delta\eta_3-(1-\sigma_3)\delta(\gamma_{A_3}+\eta_3+\mu))}{\mu(\mu+\delta)(\gamma_{A_3}+\eta_3+\mu)(g_3+\gamma_{I_3}+\mu_3+\mu)}$$

$$R_{04} = \frac{\sigma_4 \delta \beta_{A_4} \Lambda}{\mu(\mu+\delta)(\gamma_{A_4}+\eta_4+\mu)} + \frac{\beta_{I_4}\Lambda(\sigma_4\delta\eta_4-(1-\sigma_4)\delta(\gamma_{A_4}+\eta_4+\mu))}{\mu(\mu+\delta)(\gamma_{A_4}+\eta_4+\mu)(g_4+\gamma_4+\mu_4+\mu)}$$

are biologically characterized as the effect of the controls used on the four SARS-CoV-2 variants. The fundamental reproductive number R_0 is represented spectral radius of the next generation matrix FV^{-1}, which is known by $R_0 = \max\{R_{01}, R_{02}, R_{03}, R_{04}\}$

3.3 Disease free equilibrium (E^0)

we find the equilibrium point (E_0) where the population is free of disease (i.e., $E_1 = E_2 = E_3 = E_4 = A_1 = A_2 = A_3 = A_4 = I_1 = I_2 = I_3 = I_4$ = H = R = D = 0) by setting the right hand side of system (2) to zero. Then disease-free equilibrium is $E^0 = (\frac{\Lambda}{\mu}, 0, 0, 0, 0, 0, 0, 0, 0, 0, 0, 0)$.

Theorem 2. The disease-free equilibrium of system (1) is locally asymptotically stable if $R_0 < 1$,and unstable if $R_0 > 1$.

proof. The Jacobian matrix of the system (1) is given by

$J_{E^0} =$

$$\begin{pmatrix}
-\mu & 0 & -\beta_{A_1} & -\beta_{I_1} & 0 & -\beta_{A_2} & -\beta_{I_2} & 0 & -\beta_{A_3} & -\beta_{I_3} & 0 & -\beta_{A_4} & -\beta_{I_4} & 0 & 0 \\
0 & -(\mu+\delta) & 0 & \beta_{A_1} & \beta_{I_1} & 0 & \beta_{A_2} & \beta_{I_2} & 0 & \beta_{A_3} & \beta_{I_3} & 0 & \beta_{A_4} & \beta_{I_4} & 0 \\
0 & \sigma_1\delta & -X_1 & 0 & 0 & 0 & 0 & 0 & 0 & 0 & 0 & 0 & 0 & 0 & 0 \\
0 & (1-\sigma_1)\delta & \eta_1 & -Y_1 & 0 & 0 & 0 & 0 & 0 & 0 & 0 & 0 & 0 & 0 & 0 \\
0 & 0 & 0 & 0 & -(\mu+\delta) & 0 & 0 & 0 & 0 & 0 & 0 & 0 & 0 & 0 & 0 \\
0 & 0 & 0 & 0 & \sigma_2\delta & -X_2 & 0 & 0 & 0 & 0 & 0 & 0 & 0 & 0 & 0 \\
0 & 0 & 0 & 0 & (1-\sigma_2)\delta & \eta_2 & -Y_2 & 0 & 0 & 0 & 0 & 0 & 0 & 0 & 0 \\
0 & 0 & 0 & 0 & 0 & 0 & 0 & -(\mu+\delta) & 0 & 0 & 0 & 0 & 0 & 0 & 0 \\
0 & 0 & 0 & 0 & 0 & 0 & 0 & \sigma_3\delta & -X_3 & 0 & 0 & 0 & 0 & 0 & 0 \\
0 & 0 & 0 & 0 & 0 & 0 & 0 & (1-\sigma_3)\delta & \eta_3 & -Y_3 & 0 & 0 & 0 & 0 & 0 \\
0 & 0 & 0 & 0 & 0 & 0 & 0 & 0 & 0 & 0 & -(\mu+\delta) & 0 & 0 & 0 & 0 \\
0 & 0 & 0 & 0 & 0 & 0 & 0 & 0 & 0 & 0 & 0 & \sigma_4\delta & -X_4 & 0 & 0 \\
0 & 0 & 0 & 0 & 0 & 0 & 0 & 0 & 0 & 0 & (1-\sigma_4)\delta & \eta_4 & -Y_4 & 0 & 0 \\
0 & 0 & 0 & g_1 & 0 & 0 & g_2 & 0 & 0 & g_3 & 0 & 0 & g_4 & -Z & 0 \\
0 & 0 & \gamma_{A_1} & \gamma_{I_1} & 0 & \gamma_{A_2} & \gamma_{I_2} & 0 & \gamma_{A_3} & \gamma_{I_3} & 0 & \gamma_{A_4} & \gamma_{I_4} & \gamma_g & \mu
\end{pmatrix}$$

.

Where $X_i = (\gamma_{A_i} + \eta_i + \mu)$, $Y_i = (g_i + \gamma_{I_i} + \mu_i + \mu)$ and $Z = (\gamma_g + \mu_g + \mu)$ for i = 1,2,3,4.

Then -μ, -μ, -$(\gamma_g + \mu_g + \mu)$ are three eigen values of jacobian matrix and remaining 12 eigen values can be determined from the following matrix.

$$\begin{pmatrix}
-(\mu+\delta) & \beta_{A_1} & \beta_{I_1} & 0 & \beta_{A_2} & \beta_{I_2} & 0 & \beta_{A_3} & \beta_{I_3} & 0 & \beta_{A_4} & \beta_{I_4} \\
\sigma_1\delta & -X_1 & 0 & 0 & 0 & 0 & 0 & 0 & 0 & 0 & 0 & 0 \\
(1-\sigma_1)\delta & \eta_1 & -Y_1 & 0 & 0 & 0 & 0 & 0 & 0 & 0 & 0 & 0 \\
0 & 0 & 0 & -(\mu+\delta) & 0 & 0 & 0 & 0 & 0 & 0 & 0 & 0 \\
0 & 0 & 0 & \sigma_2\delta & -X_2 & 0 & 0 & 0 & 0 & 0 & 0 & 0 \\
0 & 0 & 0 & (1-\sigma_2)\delta & \eta_2 & -Y_2 & 0 & 0 & 0 & 0 & 0 & 0 \\
0 & 0 & 0 & 0 & 0 & 0 & -(\mu+\delta) & 0 & 0 & 0 & 0 & 0 \\
0 & 0 & 0 & 0 & 0 & 0 & \sigma_3\delta & -X_3 & 0 & 0 & 0 & 0 \\
0 & 0 & 0 & 0 & 0 & 0 & (1-\sigma_3)\delta & \eta_3 & -Y_3 & 0 & 0 & 0 \\
0 & 0 & 0 & 0 & 0 & 0 & 0 & 0 & 0 & -(\mu+\delta) & 0 & 0 \\
0 & 0 & 0 & 0 & 0 & 0 & 0 & 0 & 0 & \sigma_4\delta & -X_4 & 0 \\
0 & 0 & 0 & 0 & 0 & 0 & 0 & 0 & 0 & (1-\sigma_4)\delta & \eta_4 & -Y_4
\end{pmatrix}.$$

The determinant of this matrix yields an 12^{th} degree equation in λ, and analytically solving this equation requires extensive calculations. So that we use numerical methods [33] to obtain the roots because it is difficult to calculate the roots of higher-order equations analytically. By using Routh–Hurwitz Criteria [34], this disease-free equilibrium is locally asymptotically stable if $R_0 < 1$ and unstable $R_0 > 1$.

4. Model Calbiration

The results are more accurate if a model is well-fitted, which involves analyzing the fit accuracy of the model to the data. We used the SARS-CoV-2 data for India [35], which was collected between March 1, 2020, and December 20, 2021, for this investigation. The timeline of the alpha, beta, gamma, and delta variants in India is depicted in[36, 37]. By fitting the cumulative confirmed cases of the reported data in Matlab and using the least squares approach(lsqnonlin function), the 8 parameters of our proposed model have been determined. Table 1 represents the estimated and model parameter values for each variant data set. Figure.2 illustrates the fitted model with the cumulative confirmed SARS-CoV-2 cases for the alpha, beta, gamma, and delta variants. The red curve shows the model solution, and the blue curve depicts the reported data.

TABLE 1. Estimated parameter values for model (1)

Parameter	value	References	parameter	value	References
Λ	varies	-	-	-	-
δ	[0.071,0.33]	[38, 39]	-	-	-
σ_1	[0,1]	[39, 40]	γ_{A_1}	0.1511	[42, 47]
σ_2	[0,1]	[39, 40]	γ_{A_2}	0.1591	[42, 47]
σ_3	[0,1]	[39, 40]	γ_{A_3}	0.1672	[42, 47]
σ_4	[0,1]	[39, 40]	γ_{A_4}	0.1734	[42, 47]
β_{A_1}	0.2168	Fitted	γ_{I_1}	0.1401	[48, 49]
β_{A_2}	0.2331	Fitted	γ_{I_2}	0.1212	[48, 49]
β_{A_3}	0.2437	Fitted	γ_{I_3}	0.1405	[50]
β_{A_4}	0.2693	Fitted	γ_{I_4}	0.1715	[51]
β_{I_1}	0.3168	Fitted	γ_g	0.01233	[45]
β_{I_2}	0.3331	Fitted	μ_1	0.001012	[46, 52]
β_{I_3}	0.3411	Fitted	μ_2	0.001122	[46, 52]
β_{I_4}	0.3632	Fitted	μ_3	0.001473	[41, 42]
η_1	0.01435	[41, 42]	μ_4	0.017091	[41, 42]
η_2	0.01979	[41, 42]	μ_g	0.001393	[41, 42]
η_3	0.01663	[41, 42]	μ	0.0000391	[53]
η_4	0.01537	[41, 42]	R_{01}	1.1087	Fitted
g_1	0.01435	[43]	R_{02}	1.1128	Fitted
g_2	0.01979	[44]	R_{03}	1.1973	Fitted
g_3	0.01663	[43]	R_{04}	1.2646	Fitted
g_4	0.01537	[45]	R_0	1.2646	Fitted

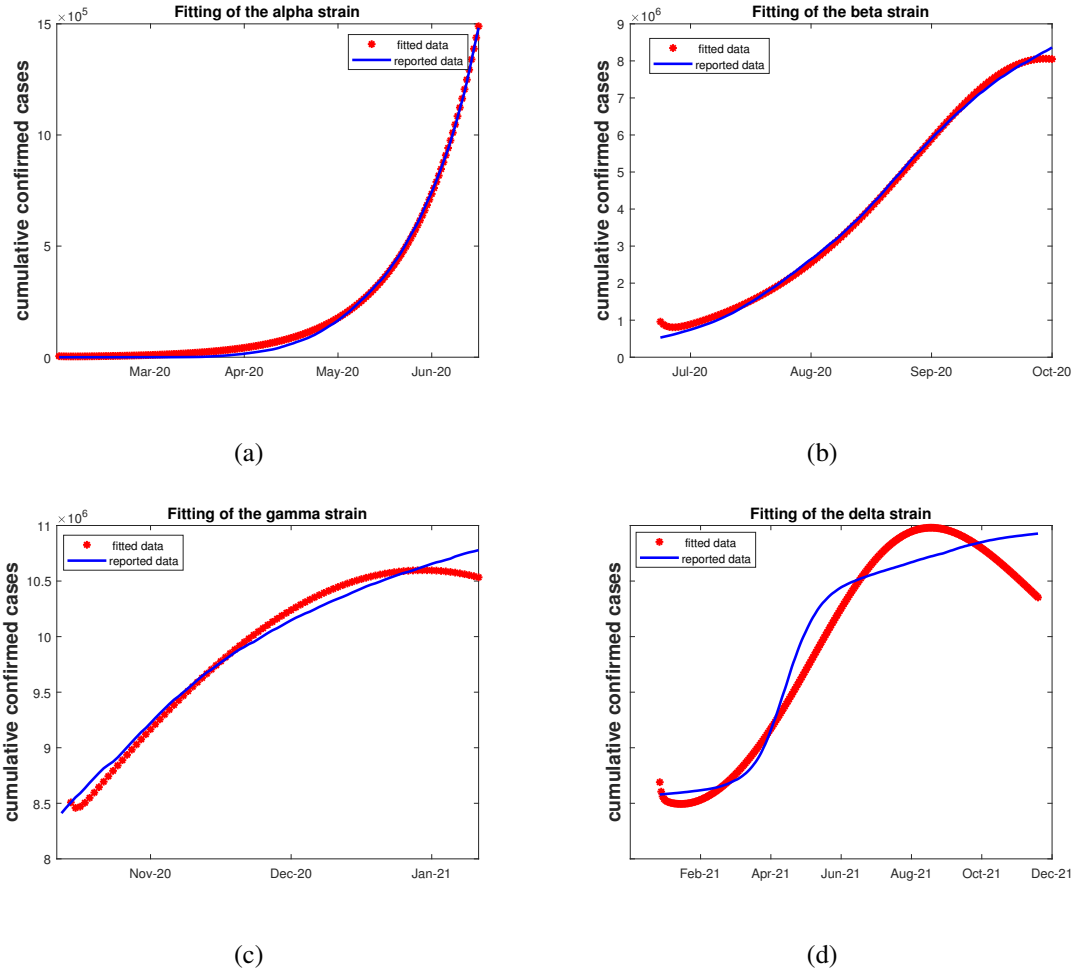

FIGURE 2. Plots showing the fitted model along with real SARS-CoV-2 cases for the alpha, beta, gamma, and delta variants in (a), (b), (c), and (d), respectively.

5. SENSITIVITY ANALYSIS

Sensitivity analysis is crucial in identifying the importance of various parameters in disease transmission. It aids in comprehending how the reproduction number value changes depending on various factors. H.S. Rodrigues et al.[54] presents a thorough study of the sensitivity to dengue fever. The ratio of the variable's relative change to the parameter's relative change is known as the normalized forward sensitivity index of a variable with respect to a parameter. Partial derivatives can also be used to define the sensitivity index when the variable is a differentiable function of the parameter. The differentiability of R_0 with respect to the particular

parameter q determines the normalized forward sensitivity index of R_0, which may be calculated as $\Gamma_q^{R_0} = \frac{\partial R_0}{\partial q} \times \frac{p}{R_0}$.

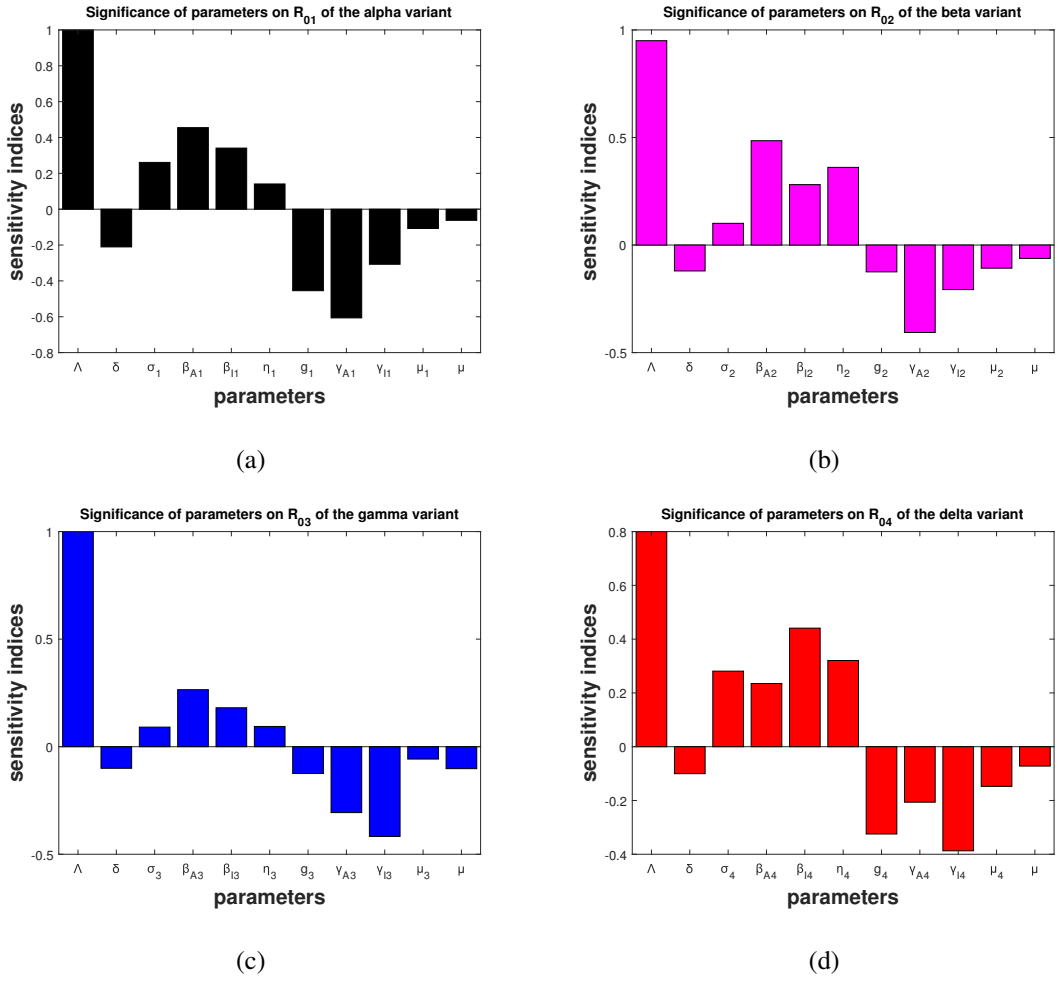

(a) (b)

(c) (d)

FIGURE 3. Normalized forward sensitivity indices of basic reproduction number with respect to various parameters for a) alpha variant, b) beta variant, c) gamma variant, and d) delta variant

Figure 3 shows the basic reproduction number's normalized forward sensitivities for the alpha, beta, gamma, and delta variants. According to Figure.3(a), the SARS-COV-2 alpha variant disease transmission rates β_{A_1} and β_{I_1} of asymptomatic and symptomatic infected individuals have positive correlations with R_{01}, whereas the recovery rates γ_{A_1} and γ_{I_1} of asymptomatic and symptomatic infected individuals have negative correlations with R_{01}. This means that the alpha variant's reproduction number R_{01} enhanced by rising the rates of β_{A_1} and β_{I_1}, but slowed down

by rising the rates γ_{A_1} and γ_{I_1}. Figure.3(b) demonstrates that the disease transmission rate β_{A_2} of beta variant and the conversion rate η_2 of asymptomatic infected individuals with beta variant to symptomatic infected individuals with beta variant have positive correlation with R_{02} while the recovery rates γ_{A_2} and γ_{I_2} have negative correlations with R_{02}. Therefore, the reproduction number R_{02} increases as the rates β_{A_2} and η_2 rises and decreases as the rates γ_{A_2} and γ_{I_2} increase. Figure. 3(c) indicates that the disease transmission rates β_{A_3} and β_{I_3} of infected individuals with gamma variant have positive correlations with R_{03} and the rates of recoveries γ_{A_3} and γ_{I_3} of infected individuals have negative correlation with R_{03}. This implies that reproduction number R_{03} increases as β_{A_3} and β_{I_3} rise and slow down as γ_{A_3} and γ_{I_3} rise. Figure.3(d) reveals that the disease transmission rate β_{A_4} of the symptomatic infected individuals with delta variant and the rate η_4 at which asymptomatic infected individuals becomes symptomatic infected with delta variant show positive correlation with R_{04} and the hospitalization rate g_4 and recovery rate γ_{I_4} of symptomatic infected individuals with delta variant shows negative correlation with R_{04}. As a result, the reproduction number R_{04} rises with rising of the rates β_{A_4} and η_4 whereas R_{04} falls with rising of g_4 and γ_{I_4} rates.

6. Optimal Control

6.1 Optimal control problem

There are numerous applications for optimal control in biology and pharmacology. It has largely been employed to study compartmental models in epidemiology. The risk of infection can be decreased by making the best use of various control measures such as Vaccination, treatment, mask use, hand washing, surface sanitization, and non-pharmaceutical interventions (public health education, isolation, and quarantine). Our primary objective is to reduce the number of contagious individuals with SARS-CoV-2 variants over a period of time [0, T] by applying the best intervention techniques. To accomplish these objectives, we provide two control variables 1) vaccination for susceptible and 2)treatment for infected and hospitalized individuals.

Vaccinated strategy for susceptible individuals: Vaccination is the most efficient technique for controlling infectious diseases. In order to stimulate the immune system of the susceptible subpopulation to recognize the pathogen and eradicate any associated microorganisms that it may come into contact with in the future, vaccines are administered to this subpopulation. This prevents the disease from spreading among susceptible people. The SARS-CoV-2 vaccines

have demonstrated up to 95% efficiency in preventing symptomatic infection. India licensed the BBV152 (Covaxin) vaccine produced by Bharat Biotech in Hyderabad and the Oxford-AstraZeneca (Covishield) vaccine produced by the Serum Institute of India in Pune in January 2021. According to a recent study [55, 56, 57], using multiple vaccinations together led to substantial improvements. The first control indicates the effort of vaccinating susceptible individuals by presuming that all susceptible individuals who have received vaccination are shifted directly to the removed class. We assume that a susceptible individual will receive both of these vaccines. we introduce these vaccination in the form of $\zeta u(t)$ where ζ is vaccination rate and u(t) is control variable that lying in between 0 and 1.

Treatment strategy for infected and hospitalized individuals: Treatment is provided to the infected and hospitalized subpopulations in order to lessen disease severity and limit infection transmission. According to studies in [58], the best treatment approach to lessen the impact of SARS-CoV-2 is the combination of immunotherapy and antiviral medications. So the second control that we take into account in this scenario is the treatment of the infected and hospitalized population. These treatments could involve the administration of immunomodulators like INF or zinc to strengthen the immune response or any recommended antiviral medications like remdesivir, arbidol, etc. that prevent viral propagation. We define the treatment for asymptomatic infected and symptomatic individuals with SARS-CoV-2 alpha, beta, gamma and delta variants in the form $\kappa_{A_i} v_{A_i}(t)$, $\kappa_{I_i} v_{I_i}(t)$ where κ_{A_i}, κ_{I_i} are the treatment rates and $v_{A_i}(t)$, $v_{I_i}(t)$ are the control variables. Also we introduce a treatment for hospitalization individuals in the form $\kappa_g v_G(t)$ whereκ_g is treatment rate and $v_G(t)$ is the control variable. Here the control variables range from 0 to 1, where 1 corresponds to a full recovery after treatment and 0 corresponds to no recovery.

Let $v = (v_{A_1}, v_{A_2}, v_{A_3}, v_{A_4}, v_{I_1}, v_{I_2}, v_{I_3}, v_{I_4}, v_g)$

Thus the admissible set of all controls is defined as

$U_{ad} = \{u(t), v(t) : 0 \leq u(t), v(t) \leq 1, \forall t \in [0, T]\ \}$.

With the objective of minimizing the cost functional, we now propose and describe the optimal

control problem using the above discussed control strategies as follows:

$$\begin{aligned}
\frac{dS}{dt} &= \Lambda - \sum_{i=1}^{4}(\beta_{A_i}A_i + \beta_{I_i}I_i)\frac{S}{N} - \zeta u(t)S - \mu S \\
\frac{dE_i}{dt} &= (\beta_{A_i}A_i + \beta_{I_i}I_i)\frac{S}{N} - (\mu+\delta)E_i \\
\frac{dA_i}{dt} &= \sigma_i\delta E_i - (\gamma_{A_i} + \eta_i + \kappa_{A_i}v_{A_i}(t) + \mu)A_i \\
\frac{dI_i}{dt} &= (1-\sigma_i)\delta E_i + \eta_i A_i - (g_i + \gamma_{I_i} + \kappa_{I_i}v_{I_i}(t) + \mu_i + \mu)I_i \\
\frac{dG}{dt} &= \sum_{i=1}^{4} g_i I_i - (\gamma_g + \kappa_g v_G(t) + \mu_g + \mu)G \\
\frac{dR}{dt} &= \sum_{i=1}^{4}(\gamma_{A_i}A_i + \gamma_{I_i}I_i) + \gamma_g G + \zeta u(t)S + \sum_{i=1}^{4}\kappa_{A_i}v_{A_i}(t)A_i(t) + \sum_{i=1}^{4}\kappa_{I_i}v_{I_i}(t)I_i(t) + \kappa_g v_G(t)G(t) - \mu R \\
\frac{dD}{dt} &= \sum_{i=1}^{4}\mu_i I_i + \mu_g G \qquad (3)
\end{aligned}$$

subject to minimize the objective functional

$$\mathscr{J} = \int_0^T (\sum_{i=1}^{4}(A_i + I_i) + \frac{B}{2}u^2 + \sum_{i=1}^{4}(\frac{C_{A_i}}{2}v_{A_i}^2 + \frac{C_{I_i}}{2}v_{I_i}^2) + \frac{C_G}{2}v_G^2)dt \qquad (4)$$

with the primary conditions expressed in Eq.(2). Here, the objective functional J depicts the total cost incurred, which is the sum of the costs listed in the integrand:

$L = \sum_{i=1}^{4}(A_i + I_i) + \frac{B}{2}u^2 + \sum_{i=1}^{4}(\frac{C_{A_i}}{2}v_{A_i}^2 + \frac{C_{I_i}}{2}v_{I_i}^2) + \frac{C_G}{2}v_G^2$

indicates the cost's current value at any time t or Lagrangian. All the parameters B, C_{A_i}, C_{I_i} and C_G for i = 1, 2, 3, 4 are non-negative and are employed as weight constants to balance the integrand's units. Additionally, they provide the estimation of the relative costs of the control functions over [0, T], which includes vaccine, treatment, and diagnosis expenses, etc. The control functions $u^*(t)$, $v_i^*(t)$, $v_{A_i}^*(t)$, $v_{I_i}^*(t)$ and $v_G^*(t)$ occur in the admissible control set U that primarily minimized the objective functional $\mathscr{J}$.

The Hamiltonian function $\mathscr{H}$ defined by

$\mathscr{H} = \sum_{i=1}^{4}(A_i + I_i) + \frac{B}{2}u^2 + \sum_{i=1}^{4}(\frac{C_{A_i}}{2}v_{A_i}^2 + \frac{C_{I_i}}{2}v_{I_i}^2) + \frac{C_G}{2}v_G^2 + \lambda_S\frac{dS}{dt} + \sum_{i=1}^{4}\lambda_{E_i}\frac{dE_i}{dt} + \sum_{i=1}^{4}\lambda_{A_i}\frac{dA_i}{dt} + \sum_{i=1}^{4}\lambda_{I_i}\frac{dI_i}{dt} + \lambda_G\frac{dG}{dt} + \lambda_R\frac{dR}{dt} + \lambda_D\frac{dD}{dt}$

where λ_S, λ_{E_i}, λ_{A_i}, λ_{I_i}, λ_G, λ_R and λ_D are the adjoint variables for i=1,2,3,4.

Theorem 3. There exist 10-tuple of optimal controls ($u^*(t)$, $v_{A_1}^*(t)$, $v_{A_2}^*(t)$, $v_{A_3}^*(t)$, $v_{A_4}^*(t)$,$v_{I_1}^*(t)$, $v_{I_2}^*(t)$, $v_{I_3}^*(t)$, $v_{I_4}^*(t)$, $v_G^*(t)$) in U_{ad} that minimizes the objective functional

$\mathscr{J}(u^*(t),v^*(t),) = \min_{u(t),v(t)\in U_{ad}} \mathscr{J}(u(t),v(t)$ corresponding to the control system (3)–(4).

proof. This theorem will be proved using [59, 60]. We have already established in Section 2 that, under the initial conditions 2 given, all solutions to 1 are nonnegative and uniformly bounded. It is clear that the objective functional is non-negative, and this indicates that the objective functional is bounded. By definition, the set of control variables, U, V, and W in U_{ad} is convex and closed. The integrand of the functional $\sum_{i=1}^{4}(A_i+I_i)+\frac{B}{2}u^2+\sum_{i=1}^{4}(\frac{C_{A_i}}{2}v_{A_i}^2+\frac{C_{I_i}}{2}v_{I_i}^2)+\frac{C_g}{2}v_G^2$ is convex on the control set U_{ad} and the state variables are bounded. As there are optimal controls for minimizing the functional subject of equations 3–4, we use Pontryagin's maximum principle [61, 62] to derive the necessary conditions to find the optimal solutions as follows:

There exists a nontrivial vector function $\lambda = \lambda_1, \lambda_2, \lambda_3,..., \lambda_n$ if (z, u) is an optimal solution of an optimal control problem and it satisfies the following equality conditions:

$\frac{dz}{dt} = \frac{\partial H(t,z,u,\lambda)}{\partial \lambda}$, $0 = \frac{\partial H(t,z,u,\lambda)}{\partial \lambda}$, and $\frac{d\lambda}{dt} = \frac{\partial H(t,z,u,\lambda)}{\partial \lambda}$.

Theorem 4. If the couple $(S^*,E_i^*,A_i^*,I_i^*,G^*,R^*,D^*)$ is the solution of the system (3) related to an optimal controls $u^*(t),v^*(t)\in U_{ad}$, then there exist adjoint functions λ_S, λ_{E_i}, λ_{A_i}, λ_{I_i}, λ_G, λ_R and λ_D satisfying the following equations:

$\frac{d\lambda_S}{dt} = -\frac{\partial \mathscr{H}}{\partial S} = \lambda_s\sum_{i=1}^{4}(\beta_{A_i}A_i+\beta_{I_i}I_i+\zeta u(t)+\mu)\frac{1}{N} + -\sum_{i=1}^{4}\lambda_{E_i}(\beta_{A_i}A_i+\beta_{I_i}I_i)\frac{1}{N}+(\lambda_S-\lambda_R)u(t)$

$\frac{d\lambda_{E_i}}{dt} = -\frac{\partial \mathscr{H}}{\partial E_i} = (\mu+\delta)\lambda_{E_i}-\sigma_i\delta\lambda_{A_i}-(1-\sigma_i)\delta\lambda_{I_i}$

$\frac{d\lambda_{A_i}}{dt} = -\frac{\partial \mathscr{H}}{\partial I_i} = -1+(\lambda_S-\lambda_{E_i})\beta_{A_i}\frac{S}{N}+\lambda_{A_i}(\gamma_{A_i}+\eta_i+\kappa_{A_i}v_{A_i}(t)+\mu)-\lambda_{I_i}\eta_i-\lambda_R(\gamma_{A_i}+\kappa_{A_i}v_{A_i}(t))$

$\frac{d\lambda_{I_i}}{dt} = -\frac{\partial \mathscr{H}}{\partial I_i} = -1+(\lambda_S-\lambda_{E_i})\beta_{I_i}\frac{S}{N}+\lambda_{I_i}(\gamma_{A_i}+g_i+\kappa_{I_i}v_{I_i}(t)+\mu_i+\mu)-\lambda_G g_i-\lambda_R(\gamma_{I_i}+\kappa_{I_i}v_{I_i}(t))-\lambda_D\mu_g$

$\frac{d\lambda_H}{dt} = -\frac{\partial \mathscr{H}}{\partial G} = \lambda_G(\gamma_g+\mu_g+\kappa_g v_G+\mu)-\lambda_R(\gamma_g+\kappa_G v_G)-\lambda_D\mu_g$

$\frac{d\lambda_R}{dt} = -\frac{\partial \mathscr{H}}{\partial R} = \mu\lambda_R$

$\frac{d\lambda_D}{dt} = 0$

with the transversality conditions at time T: $\lambda_S(T)=0$, $\lambda_{E_i}(T)=0$, $\lambda_{A_i}(T)=0$, $\lambda_{I_i}(T)=0$, $\lambda_G(T)=0$, $\lambda_R(T)=0$ and $\lambda_D(T)=0$.

Moreover for $t\in[0,T]$, the optimal controls $u^*(t)$, and $v_{A_i}^*(t)$, $v_{I_i}^*(t)$ and $v_G^*(t)$ determined by

$u^*(t) = \min\{1,\max\{0,\frac{(\lambda_S-\lambda_R)\zeta S}{B}\}\}$,

$v_{A_i}^*(t) = \min\{1,\max\{0,\frac{(\lambda_{A_i}-\lambda_R)\kappa_{A_i}A_i}{C_{A_i}}\}\}$,

$v_{I_i}^*(t) = \min\{1,\max\{0,\frac{(\lambda_{I_i}-\lambda_R)\kappa_{I_i}I_i}{C_{I_i}}\}\}$ and

$v_G^*(t) = \min\{1, \max\{0, \frac{(\lambda_G - \lambda_R)\kappa_g G}{C_G}\}\}$

proof. The Hamiltonian function $\mathscr{H}$ for this optimal control system is defined by

$\mathscr{H} = \sum_{i=1}^4 (A_i + I_i) + \frac{B}{2}u^2 + \sum_{i=1}^4 (\frac{C_{A_i}}{2}v_{A_i}^2 + \frac{C_{I_i}}{2}v_{I_i}^2) + \frac{C_g}{2}v_G^2 + \lambda_S(\Lambda - \sum_{i=1}^4 (\beta_{A_i}A_i + \beta_{I_i}I_i)\frac{S}{N} - \zeta u(t) - \mu S) + \sum_{i=1}^4 \lambda_{E_i}((\beta_{A_i}A_i + \beta_{I_i}I_i)\frac{S}{N} - (\mu+\delta)E_i) + \sum_{i=1}^4 \lambda_{A_i}(\sigma_i\delta E_i - (\gamma_{A_i} + \eta_i + \kappa_{A_i}v_{A_i}(t) + \mu)A_i) + \sum_{i=1}^4 \lambda_{I_i}((1-\sigma_i)\delta E_i + \eta_i A_i - (g_i + \gamma_{I_i} + \kappa_{I_i}v_{I_i}(t) + \mu_i + \mu)I_i) + \lambda_G(\sum_{i=1}^4 g_i I_i - (\gamma_g + \kappa_g v_G(t) + \mu_g + \mu)G) + \lambda_R(\sum_{i=1}^4 (\gamma_{A_i}A_i + \gamma_{I_i}I_i) + \gamma_g G + \zeta u(t) + \sum_{i=1}^4 (\kappa_{A_i}v_{A_i}(t) + \kappa_{I_i}v_{I_i}(t)) + \kappa_g v_G(t) - \mu) + \lambda_D(\sum_{i=1}^4 \mu_i I_i + + \mu_g G)$

Using Pontryagin's maximal principle, the following canonical expressions are satisfied by the co-state variables :

$\frac{d\lambda_S}{dt} = -\frac{\partial \mathscr{H}}{\partial S}$, $\lambda_S(T) = 0$,
$\frac{d\lambda_{E_i}}{dt} = -\frac{\partial \mathscr{H}}{\partial E_i}$, $\lambda_{E_i}(T) = 0$,
$\frac{d\lambda_{A_i}}{dt} = -\frac{\partial \mathscr{H}}{\partial A_i}$, $\lambda_{A_i}(T) = 0$,
$\frac{d\lambda_{I_i}}{dt} = -\frac{\partial \mathscr{H}}{\partial I_i}$, $\lambda_{I_i}(T) = 0$,
$\frac{d\lambda_H}{dt} = -\frac{\partial \mathscr{H}}{\partial H}$, $\lambda_G(T) = 0$,
$\frac{d\lambda_R}{dt} = -\frac{\partial \mathscr{H}}{\partial R}$, $\lambda_R(T) = 0$.
$\frac{d\lambda_D}{dt} = -\frac{\partial \mathscr{H}}{\partial D}$, $\lambda_D(T) = 0$.

Now, the optimality conditions $\frac{\partial \mathscr{H}}{\partial u} = 0$, $\frac{\partial \mathscr{H}}{\partial v_{A_i}} = 0$, $\frac{\partial \mathscr{H}}{\partial v_{I_i}} = 0$ and $\frac{\partial \mathscr{H}}{\partial v_G} = 0$ are used to illustrate the optimal controls $u^*(t)$, $v_{A_i}^*(t)$, $v_{I_i}^*(t)$ and $v_G^*(t)$ where i=1,2,3,4.

$\frac{\partial \mathscr{H}}{\partial u} = P_i u_i - \lambda_S \zeta S + \lambda_R \zeta S = 0$
$\Rightarrow u = \frac{(\lambda_S - \lambda_R)\zeta_i S}{B}$
$\frac{\partial \mathscr{H}}{\partial v_{A_i}} = C_{A_i}v_{A_i} - \lambda_{A_i}\kappa_{A_i}A_i + \lambda_R\kappa_{A_i}A_i = 0$
$\Rightarrow v_{A_i} = \frac{(\lambda_{A_i} - \lambda_R)\kappa_{A_i}A_i}{C_{A_i}}$
$\frac{\partial \mathscr{H}}{\partial v_{I_i}} = C_{I_i}v_{I_i} - \lambda_{I_i}\kappa_{I_i}I_i + \lambda_R\kappa_{I_i}I_i = 0$
$\Rightarrow v_{I_i} = \frac{(\lambda_{I_i} - \lambda_R)\kappa_{I_i}I_i}{C_{I_i}}$
$\frac{\partial \mathscr{H}}{\partial v_G} = C_G v_G - \lambda_G\kappa_g G + \lambda_R\kappa_g G = 0$
$\Rightarrow v_G = \frac{(\lambda_G - \lambda_R)\kappa_g G}{C_G}$

The equations $u^*(t)$, $v_{A_i}^*(t)$, $v_{I_i}^*(t)$ and $v_G^*(t)$ can be easily obtained using the bounds of the controls in U_{ad}.

6.2 Optimal control model simulation

In this section, we conduct a numerical analysis to comprehend the effectiveness of vaccination and treatment strategies over time. This is achieved by investigating the influence of optimal controls on the dynamics of the system (3). we apply the fourth-order Runge-Kutta method to study the numerical simulation of the system of differential equations (3) with the help of MATLAB software. Using forward difference approximation, system (3) was solved. then, the adjoint system (4) was resolved using backward difference approximation because of the transversality constraints. For the simulation, we use a period of 300 days. We use the initial conditions S(0) = 1215263184, $E_1(0) = 47000$, $A_1(0) = 1$, $I_1(0) = 1$, $E_2(0) = 43000$, $I_2(0) = 19429$, $A_2(0) = 21602$, $E_3(0) = 40500$, $A_3(0) = 50034$, $I_3(0) = 45928$, $E_4(0) = 40000$, $A_4(0) = 27086$, $I_4(0) = 17015$, G(0) = 5000, R(0) = 1000 and D(0)=200 and the parameters listed in Table 1 to solve the controlled system(3) and the related adjoint system(4). The positive weight constant B is taken as 10^6 based on the analysis in[58]. For the treatment of the infected and hospitalised populations, we assume the treatment rate for each the variant is 0.3 and that the values of weight constants C_{A_i}, C_{I_i} for i=1,2,3,4 and C_g are 1000, 1000 and 500 respectively. Because we assume that all hospital facilities are available, the weight constant associated with the total cost of applying the treatment strategy for the hospitalised population is considered to be lower than that for treating the infected population with the four variants of SARS-CoV-2. Three different strategies were implemented in the numerical simulations. We plot the graphs for each variant in each strategy by combining the asymptomatic infected and symptomatic infected individuals.

Strategy A: We analyse the impact of the SARS-COV-2 vaccination for the susceptible populations. The control u control is used to fulfill these objectives. Figure 4 showed the significant differences in the populations with SARS-COV-2 alpha, beta, gamma, and delta variant infections in the presence of control and in the absence of controls. Here the number of infected population with alpha variant decreases from 7.71×10^6 to 3.47×10^6, with beta variant reduces from 1.83×10^7 to 0.75×10^7, with gamma variant reduces from 4.35×10^7 to 2.11×10^7 and delta variant reduces from 5.72×10^7 to 2.27×10^7 after the control was executed.

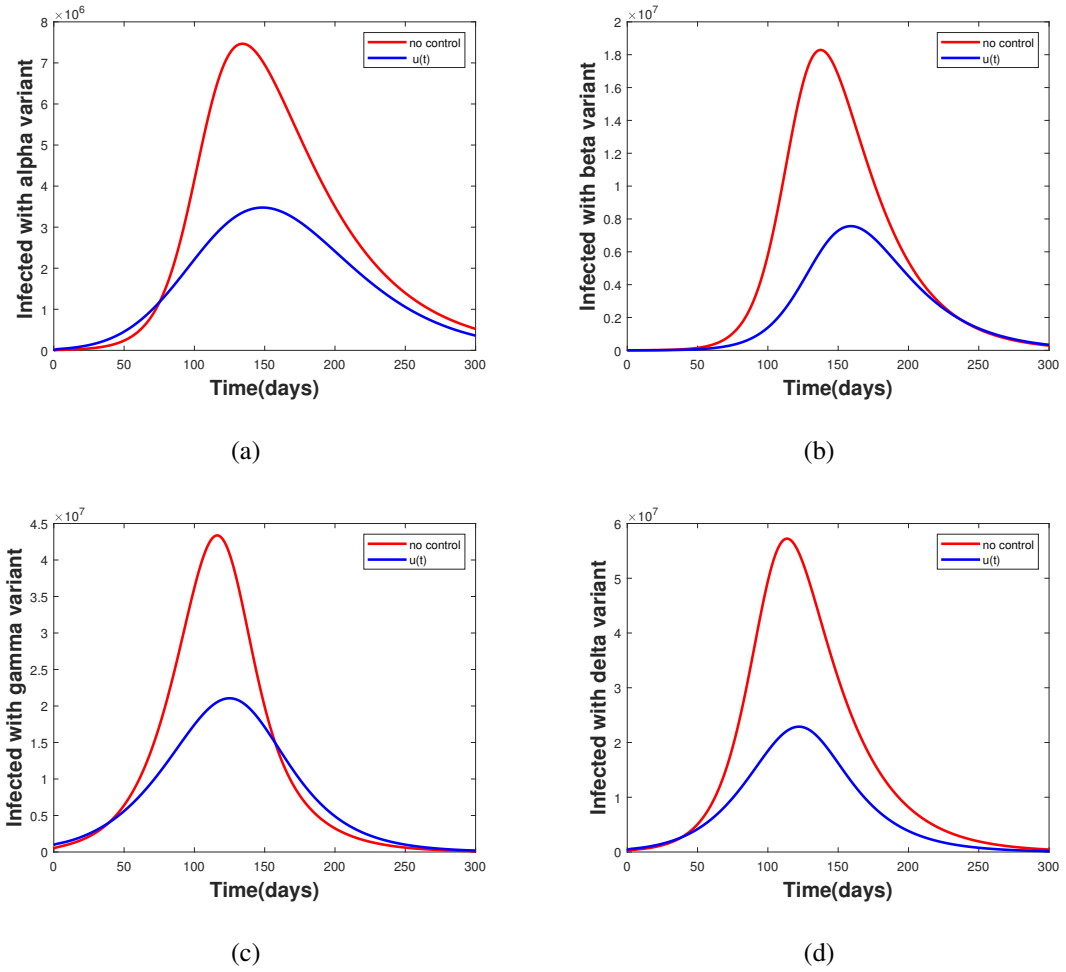

FIGURE 4. Comparisons between the infected individuals with SARS-COV-2 alpha variant, beta variant, gamma variant, and delta variant in relation to the control u(t).

Strategy B: we evaluate the impact of optimal treatment for infected individuals with SARS-COV-2 alpha, beta, gamma and delta variants in reducing the infected individuals. The only control used to achieve this is v. Figure 5 demonstrated the statistically significant differences between the SARS-COV-2 alpha, beta, gamma, and delta variant infected populations with control u and the case when there is no control. Here, at the conclusion of the application of control v the number of infected population with the alpha variant decreases from 7.71×10^6 to 4.21×10^6, with beta variant decreases from 1.83×10^7 to 1.01×10^7 , with gamma variant decreases from 4.35×10^7 to 2.83×10^7 and delta variant decreases from 5.72×10^7 to 3.46×10^7.

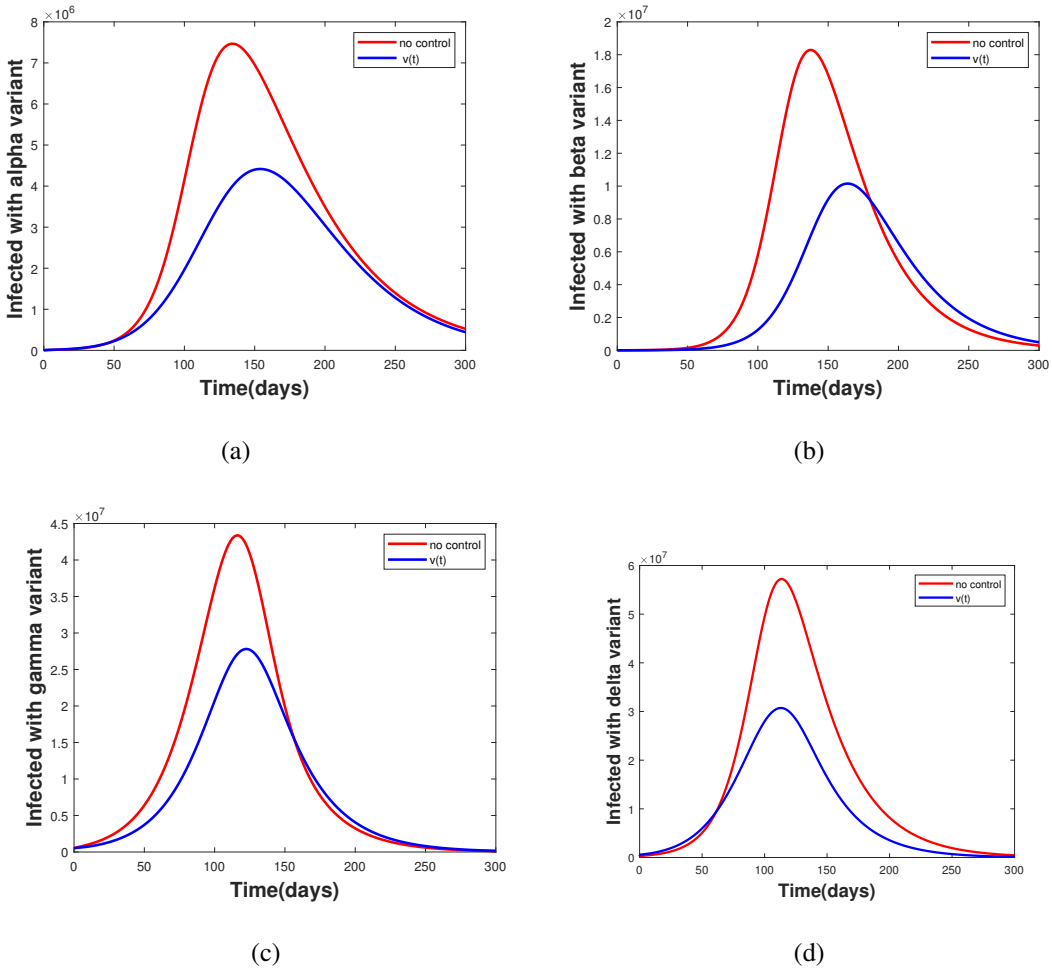

FIGURE 5. Comparisons between the infected individuals with SARS-COV-2 alpha variant, beta variant, gamma variant, and delta variant in relation to the control v(t).

Strategy C: We examine the effectiveness of SARS-COV-2 vaccine for the susceptible population, and the impact of optimal treatment for infected individuals with SARS-COV-2 alpha, beta, gamma and delta variants in reducing the infected individuals. By combining the controls u and v, these objectives can be attained. The SARS-COV-2 alpha, beta, gamma, and delta variant infected populations with controls u and v were significantly different from those with no controls, as shown in Figure 6. Here the number of infected population with alpha variant falls from 7.71×10^6 to 1.59×10^6, with beta variant falls from 1.83×10^7 to 0.34×10^7, with

gamma variant decreases 4.35×10^7 to 0.95×10^7 and delta variant falls from 5.72×10^7 to 1.55×10^7 at the end of the implementation of the controls u and v.

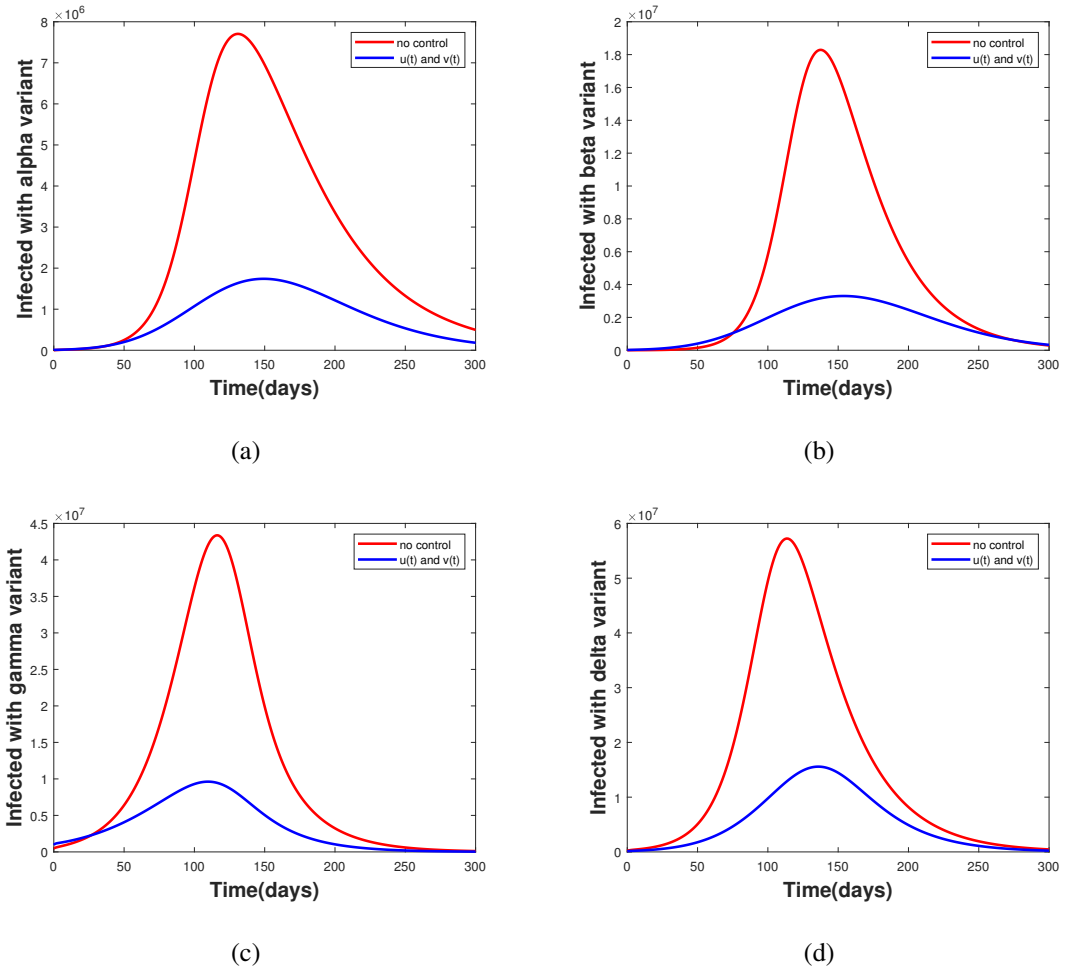

FIGURE 6. Comparisons of the corresponding to the infected individuals with (a) alpha variant (b) beta variant (c) gamma variant and (d) delta variant with respect to controls u(t) and v(t).

The combination of two controls, u and v is more effective than the single control u and single control v in reducing the number of SARS-COV-2 alpha, beta, gamma, and delta infected individuals, as shown in the figures above 4, 5 and 6.

6.3 Cost-effectiveness analysis

We analyse and evaluate the four strategies cost-effectiveness in order to determine the most effective cost-effective strategy. In order to study cost-effectiveness analyses, the incremental cost effectiveness ratio (ICER) is used [61, 62]. Any two different disease-prevention strategies

can be compared using ICER if they have different costs and health outcomes. The ICER of any two different strategies i and j is calculated as follows:

$$ICER = \frac{\text{Difference in total cost of strategies i and j}}{\text{Difference in total averted infections of strategies i and j}}$$

The total cost for each combined effort of the control strategies is computed from the objective functional 4, while the total number of infections averted is determined by comparing the number of infected individuals without and with control measures. The numerical results for the control measures are shown in Table 2 and are arranged in increasing order of infection averted.

TABLE 2. Total averted infections and total costs for strategies A, B and C

Strategy	Total averted infections (TA)	Total cost (TC)
B	4.01×10^6	4.85×10^5
A	4.75×10^7	4.21×10^5
C	5.42×10^7	3.57×10^5

The ICER values are calculated as by computing the following formula for any two distinct strategies, i and j, where strategy j is more successful than strategy i:

$$ICER(i) = \frac{\text{Total cost in strategy i}}{\text{Total averted infections in strategy i}}$$

$$ICER(j) = \frac{\text{Difference in total cost in strategies i and j}}{\text{Difference in total averted infections in strategies i and j}}$$

The fact that strategy i has a high ICER shows that it is both more expensive and less efficient than strategy j. The lower ICER for strategy i shows that it is strongly dominant.
The ICER for strategies C and B is calculated, and the results are compared in Table 3.

TABLE 3. Total infection averted, total cost and ICER

Strategy	Total averted infections (TA)	Total cost (TC)	ICER
B	4.01×10^7	4.85×10^5	0.0086
C	5.42×10^7	3.57×10^5	0.0065

$ICER(C) = \frac{3.57\times10^5}{5.42\times10^7} = 0.0065$ and $ICER(B) == \frac{1.25\times10^5}{1.41\times10^7} = 0.0089$

Since $ICER(C) < ICER(B)$, Strategy C is less efficient than strategy B. As a result, option B is taken out of the competition.

Now, as shown in Table 4, the strategies C and A are compared.

TABLE 4. Total infection averted, total cost and ICER

Strategy	Total averted infections (TA)	Total cost (TC)	
A	4.75×10^7	4.21×10^5	0.0096
C	5.42×10^7	3.57×10^5	0.0065

$ICER(C) = \frac{3.57\times10^5}{5.42\times10^7} = 0.0065$ and $ICER(A) == \frac{0.64\times10^5}{0.67\times10^7} = 0.0096$

Due to the fact that $ICER(C) < ICER(A)$, strategy C is less effective than strategy A. Following that, option C is eliminated from the list of possibilities.

Based on this, we get to the conclusion that the strategy C which includes the use of vaccination for susceptible individuals as well as treatment for infected individuals with SARS-COV-2 alpha, beta, gamma, and delta variants has a least ICER and is therefore the most effective strategy.

7. CONCLUSION

To better understand how various viruses move within and between individuals, mathematical modelling in association with mathematical analysis is a useful technique. Thus, understanding the dynamics of numerous infectious diseases is possible. In light of the complexity of how viruses spread in a population, mathematical models often can provide insights that are difficult to anticipate. In this study, we developed a deterministic model to study the transmission dynamics of four different SARS-CoV-2 variants, each of which is infectious differently.

First, the proposed model's positivity and boundedness are verified, and then the model's local stability analysis is carried out by employing the next-generation matrix approach. We determined that the fundamental reproduction number is defined by the maximum of the following four threshold quantities: R_{01}, R_{02}, R_{03}, and R_{04}. A thorough analysis of sensitivity is performed in this work by using the normalized forward sensitivity index of the basic reproduction number for four SARS-COV-2 variants independently. Limiting contact, sanitizing, isolating, and hospitalization all have a significant impact on the dynamics of SARS-CoV-2 transmission and can substantially slow the spread of SARS-CoV-2 variants. So, it is essential to encourage the population to get the vaccine and visit hospitals for treatment. Due to these factors, we implement an optimum control problem for the proposed model over the period of 300 days that considered the effects of vaccination and treatment strategies on four SARS-CoV-2 variants transmission. Numerical simulations for four SARS-CoV-2 variants are performed with the combination of single control strategies and two control strategies. The numerical analysis demonstrates that every strategy has the ability to reduce the spread of the disease. It was observed that the combination of vaccination and treatment strategies gave the best outcome in reducing the peaks of infection with four variants. Additionally, the cost-effectiveness analysis reveals that the strategy C, which includes vaccination for the susceptible population and treatment for SARS-COV-2 infected individuals with alpha, beta, gamma, and delta, is the most effective. We believe that this research will assist policymakers to better understand how vaccination and treatment work as control measures among SARS-CoV-2 infected population with alpha, beta, gamma, and delta variants. It will also assist in the development of strategies that will effectively reduce the COVID-19 pandemic's spread.

CONFLICT OF INTERESTS

The authors declare that there is no conflict of interests.

REFERENCES

[1] World Health Organization, Coronavirus disease (COVID-19) pandemic, https://www.who.int/emergencies/diseases/novel-coronavirus-2019.

[2] CDC, SARS-CoV-2 variant classifications and definitions, https://www.cdc.gov/coronavirus/2019-ncov/variants/variant-classifications.html.

[3] National Collaborating Centre for Infectious Diseases, Updates on COVID-19 variants, https://nccid.ca/covid-19-variants/.

[4] V. Hill, L. Du Plessis, T.P. Peacock, et al. The origins and molecular evolution of SARS-CoV-2 lineage B.1.1.7 in the UK, Virus Evol. 8 (2022), veac080. https://doi.org/10.1093/ve/veac080.

[5] P.D. Yadav, P. Sarkale, A. Razdan, et al. Isolation and characterization of SARS-CoV-2 Beta variant from UAE travelers, J. Infect. Public Health. 15 (2022), 182-186. https://doi.org/10.1016/j.jiph.2021.12.011.

[6] J.F. da Silva, R.J. Esteves, C. Siza, et al. Cluster of SARS-CoV-2 gamma variant infections, Parintins, Brazil, March 2021, Emerg. Infect. Dis. 28 (2022), 262-264. https://doi.org/10.3201/eid2801.211817.

[7] G. Novelli, V. Colona, P. Pandolfi, A focus on the spread of the delta variant of SARS-CoV-2 in India, Indian J. Med. Res. 153 (2021), 537-541. https://doi.org/10.4103/ijmr.ijmr_1353_21.

[8] M. Mohsin, S. Mahmud, Omicron SARS-CoV-2 variant of concern, Medicine. 101 (2022), e29165. https://doi.org/10.1097/md.0000000000029165.

[9] J.D. Murray, Mathematical biology I: An introduction, third edition. Interdisciplinary applied mathematics, Springer, New York, USA, (2021).

[10] F. Brauer, C. Castillo-Chavez, Mathematical models in population biology and epidemiology, in: Tests in Applied Mathematics, Volume 40, Springer, New York, (2001).

[11] S. Kim, J. Lee, E. Jung, Mathematical model of transmission dynamics and optimal control strategies for 2009 A/H1N1 influenza in the Republic of Korea, J. Theor. Biol. 412 (2017), 74-85. https://doi.org/10.1016/j.jtbi.2016.09.025.

[12] S. He, S. Tang, L. Rong, A discrete stochastic model of the COVID-19 outbreak: Forecast and control, Math. Biosci. Eng. 17 (2020), 2792-2804. https://doi.org/10.3934/mbe.2020153.

[13] D. Faranda, T. Alberti, Modeling the second wave of COVID-19 infections in France and Italy via a stochastic SEIR model, Chaos. 30 (2020), 111101. https://doi.org/10.1063/5.0015943.

[14] S. Kurmi, U. Chouhan, A multicompartment mathematical model to study the dynamic behaviour of COVID-19 using vaccination as control parameter, Nonlinear Dyn. 109 (2022), 2185-2201. https://doi.org/10.1007/s11071-022-07591-4.

[15] Z.S. Kifle, L.L. Obsu, Mathematical modeling for COVID-19 transmission dynamics: A case study in Ethiopia, Results Phys. 34 (2022), 105191. https://doi.org/10.1016/j.rinp.2022.105191.

[16] I. Darti, Trisilowati, M. Rayungsari, et al. A SEIQRD epidemic model to study the dynamics of COVID-19 disease, Commun. Math. Biol. Neurosci. 2023 (2023), 5. https://doi.org/10.28919/cmbn/7822.

[17] S.R. Bandekar, M. Ghosh, Mathematical modeling of COVID-19 in India and its states with optimal control, Model. Earth Syst. Environ. 8 (2021), 2019-2034. https://doi.org/10.1007/s40808-021-01202-8.

[18] B. Chhetri, D.K.K. Vamsi, D.B. Prakash, et al. Age Structured Mathematical Modeling Studies on COVID-19 with respect to Combined Vaccination and Medical Treatment Strategies, Comput. Math. Biophys. 10 (2022), 281-303. https://doi.org/10.1515/cmb-2022-0143.

[19] D. Kada, A. Kouidere, O. Balatif, et al. Mathematical modeling of the spread of COVID-19 among different age groups in Morocco: Optimal control approach for intervention strategies, Chaos Solitons Fractals. 141 (2020), 110437. https://doi.org/10.1016/j.chaos.2020.110437.

[20] O. Yagan, A. Sridhar, R. Eletreby, et al. Modeling and analysis of the spread of COVID-19 under a multiple-strain model with mutations, Harvard Data Sci. Rev. Spec. Iss. 1 (2021), 1-31. https://doi.org/10.1162/9960 8f92.a11bf693.

[21] E.F. Arruda, S.S. Das, C.M. Dias, et al. Modelling and optimal control of multi strain epidemics, with application to COVID-19, PLoS ONE. 16 (2021), e0257512. https://doi.org/10.1371/journal.pone.0257512.

[22] M. Massard, R. Eftimie, A. Perasso, et al. A multi-strain epidemic model for COVID-19 with infected and asymptomatic cases: Application to French data, J. Theor. Biol. 545 (2022), 111117. https://doi.org/10.101 6/j.jtbi.2022.111117.

[23] G. Gonzalez-Parra, D. Martínez-Rodríguez, R. Villanueva-Micó, Impact of a new SARS-CoV-2 variant on the population: a mathematical modeling approach, Math. Comput. Appl. 26 (2021), 25. https://doi.org/10.3 390/mca26020025.

[24] D. Bentaleb, S. Harroudi, S. Amine, et al. Analysis and optimal control of a multistrain SEIR epidemic model with saturated incidence rate and treatment, Differ. Equ. Dyn. Syst. (2020). https://doi.org/10.1007/s12591-0 20-00544-6.

[25] A. Essounaini, A. Labzai, H. Laarabi, et al. Mathematical modeling and optimal control strategy for a discrete time model of COVID-19 variants, Commun. Math. Biol. Neurosci. 2022 (2022), 25. https://doi.org/10.289 19/cmbn/6886.

[26] R.A. Sari, U. Habibah, A. Widodo, Optimal control on model of SARS disease spread with vaccination and treatment, J. Exp. Life Sci. 7 (2017), 61-68. https://doi.org/10.21776/ub.jels.2017.007.02.01.

[27] B. Khajji, L. Boujallal, O. Balatif, et al. Mathematical modelling and optimal control strategies of a multi-strain COVID-19 spread, J. Appl. Math. 2022 (2022), 9071890. https://doi.org/10.1155/2022/9071890.

[28] O.J. Watson, G. Barnsley, J. Toor, et al. Global impact of the first year of COVID-19 vaccination: a mathematical modelling study, Lancet Infect. Dis. 22 (2022), 1293-1302. https://doi.org/10.1016/s1473-3099(22)0 0320-6.

[29] J. Koshy, Coronavirus — Updated data from Covaxin phase 3 trial shows 78% efficacy ,(2021). https://www.thehindu.com/sci-tech/health/updated-data-from-covaxin-phase-3-trial-shows-78-efficacy/article3437601 8.ece.

[30] S. Pramod, D. Govindan, P. Ramasubramani, et al. Effectiveness of Covishield vaccine in preventing Covid-19 - A test-negative case-control study, Vaccine. 40 (2022), 3294-3297. https://doi.org/10.1016/j.vaccine.2022.02.014.

[31] P. van den Driessche, J. Watmough, Reproduction numbers and sub-threshold endemic equilibria for compartmental models of disease transmission, Math. Biosci. 180 (2002), 29-48. https://doi.org/10.1016/s0025-5564(02)00108-6.

[32] O.Diekmann, J.A.P. Heesterbeek, Mathematical epidemiology of infectious diseases: model building, analysis and interpretation, Wiley series in mathematical and computational biology, Wiley, (2000).

[33] L. Wamg, K. Wang, G. Zhou, Numerical methods for solving high order polynomial equations, in: 2011 Fourth International Conference on Information and Computing, Phuket, Thailand, 150-153, (2011).

[34] https://www.sciencedirect.com/topics/engineering/routh-hurwitz-criterion.

[35] https://data.covid19india.org

[36] https://www.livemint.com/news/world/omicron-variant-xbb-makes-up-63-of-covid-cases-reported-in-india-11672767226577.html.

[37] J. Singh, S.A. Rahman, N.Z. Ehtesham, et al. SARS-CoV-2 variants of concern are emerging in India, Nat. Med. 27 (2021), 1131-1133. https://doi.org/10.1038/s41591-021-01397-4.

[38] S.A. Lauer, K.H. Grantz, Q. Bi, et al. The incubation period of coronavirus disease 2019 (COVID-19) from publicly reported confirmed cases: estimation and application, Ann. Intern. Med. 172 (2020), 577-582. https://doi.org/10.7326/m20-0504.

[39] R. Li, S. Pei, B. Chen, et al. Substantial undocumented infection facilitates the rapid dissemination of novel coronavirus (SARS-CoV-2), Science. 368 (2020), 489-493. https://doi.org/10.1126/science.abb3221.

[40] N. Ferguson, D. Laydon, G. Nedjati Gilani, et al. Report 9: Impact of non-pharmaceutical interventions (NPIs) to reduce COVID19 mortality and healthcare demand, Imperial College London, 2020. https://doi.org/10.25561/77482.

[41] S.R. Bandekar, M. Ghosh, Mathematical modeling of COVID-19 in India and Nepal with optimal control and sensitivity analysis, Eur. Phys. J. Plus. 136 (2021), 1058. https://doi.org/10.1140/epjp/s13360-021-02046-y.

[42] S.K. Ghosh, S. Ghosh, A mathematical model for COVID-19 considering waning immunity, vaccination and control measures, Sci. Rep. 13 (2023), 3610. https://doi.org/10.1038/s41598-023-30800-y.

[43] R.K. Rai, S. Khajanchi, P.K. Tiwari, et al. Impact of social media advertisements on the transmission dynamics of COVID-19 pandemic in India, J. Appl. Math. Comput. 68 (2021), 19-44. https://doi.org/10.1007/s12190-021-01507-y.

[44] S. Khajanchi, K. Sarkar, J. Mondal, et al. Mathematical modeling of the COVID-19 pandemic with intervention strategies, Results Phys. 25 (2021), 104285. https://doi.org/10.1016/j.rinp.2021.104285.

[45] S.S. Negi, P.S. Rana, N. Sharma, et al. A novel SEIAHR compartment model for accessing the impact of vaccination, intervention policies, and quarantine on the COVID-19 pandemic: a case study of most affected countries Brazil, India, Italy, and USA, Comput. Appl. Math. 41 (2022), 305. https://doi.org/10.1007/s40314-022-01993-1.

[46] A. Tripathi, R.N. Tripathi, D. Sharma, A mathematical model to study the COVID-19 pandemic in India, Model. Earth Syst. Environ. 8 (2021), 3047-3058. https://doi.org/10.1007/s40808-021-01280-8.

[47] A. Singh, M. Arquam, Epidemiological modeling for COVID-19 spread in India with the effect of testing, Physica A: Stat. Mech. Appl. 592 (2022), 126774. https://doi.org/10.1016/j.physa.2021.126774.

[48] S. Khajanchi, K. Sarkar, Forecasting the daily and cumulative number of cases for the COVID-19 pandemic in India, Chaos. 30 (2020), 071101. https://doi.org/10.1063/5.0016240.

[49] T. Sardar, S.S. Nadim, S. Rana, et al. Assessment of lockdown effect in some states and overall India: A predictive mathematical study on COVID-19 outbreak, Chaos Solitons Fractals. 139 (2020), 110078. https://doi.org/10.1016/j.chaos.2020.110078.

[50] M.A. Rao, A. Venkatesh, SEAIQHRDP mathematical model Analysis for the transmission dynamics of COVID-19 in India, J. Comput. Anal. Appl. 31 (2023), 96-116.

[51] Shyamsunder, S. Bhatter, K. Jangid, et al. A new fractional mathematical model to study the impact of vaccination on COVID-19 outbreaks, Decision Anal. J. 6 (2023), 100156. https://doi.org/10.1016/j.dajour.2022.100156.

[52] V.P. Bajiya, S. Bugalia, J.P. Tripathi, Mathematical modeling of COVID-19: Impact of non-pharmaceutical interventions in India, Chaos. 30 (2020), 113143. https://doi.org/10.1063/5.0021353.

[53] https://www.mygov.in/covid-19.

[54] H.S. Rodrigues, M.T.T. Monteiro, D.F.M. Torres, Sensitivity analysis in a dengue epidemiological model, Conf. Papers Math. 2013 (2013), 721406. https://doi.org/10.1155/2013/721406.

[55] E. Callaway, Mix-and-match COVID vaccines trigger potent immune response, Nature. 593 (2021), 491-491. https://doi.org/10.1038/d41586-021-01359-3.

[56] V.P. Chavda, D.R. Vihol, H.K. Solanki, et al. The vaccine world of COVID-19: India's contribution, Vaccines. 10 (2022), 1943. https://doi.org/10.3390/vaccines10111943.

[57] Satvik, S. Chakole, K.H. Reddy, Comparison of efficacy of various COVID-19 vaccines available in India, J. Res. Med. Dent. Sci. 10 (2022), 127-132.

[58] B. Chhetri, V.M. Bhagat, D.K.K. Vamsi, et al. Within-host mathematical modeling on crucial inflammatory mediators and drug interventions in COVID-19 identifies combination therapy to be most effective and optimal, Alexandria Eng. J. 60 (2021), 2491-2512. https://doi.org/10.1016/j.aej.2020.12.011.

[59] L.S. Pontryagin, V.G. Boltyanskii, R.V. Gamkrelidze, et al. The mathematical theory of optimal processes, Interscience Publishers, New York, 1962.

[60] S. Lenhart, J.T. Workman, Optimal control applied to biological models. Mathematical and Computational Biology Series, Chapman & Hall/CRC, London, 2007.

[61] S. Olaniyi, O.S. Obabiyi, K.O. Okosun, et al. Mathematical modelling and optimal cost-effective control of COVID-19 transmission dynamics, Eur. Phys. J. Plus. 135 (2020), 938. https://doi.org/10.1140/epjp/s13360-020-00954-z.

[62] Y. Deng, Y. Zhao, Mathematical modeling for COVID-19 with focus on intervention strategies and cost-effectiveness analysis, Nonlinear Dyn. 110 (2022), 3893-3919. https://doi.org/10.1007/s11071-022-07777-w.